ACS OMEGA

Open Access

http://pubs.acs.org/journal/acsodf

Article

Fibrillar Alpha-Synuclein Alters the Intracellular Chaperone Levels within Hours of Its Internalization

Tugay Çamoğlu, Zuhal Yurttaş, Ümit Yaşar Kına, Pınar Akkuş Süt, Fikrettin Sahin, Erdinç Dursun, and Duygu Gezen-Ak*

Cite This: *ACS Omega* 2024, 9, 17185−17194

Read Online

ACCESS | Metrics & More | Article Recommendations | Supporting Information

ABSTRACT: Parkinson's disease (PD) is the second most prevalent neurodegenerative disorder worldwide. According to the Braak hypothesis, the disease spreads along specific neuroanatomical pathways. Studies indicate that fibrillar alpha-synuclein (F-αSyn) can propagate from cell-to-cell by following intercellular connections, leading to the selective death of certain cell groups like substantia nigra dopaminergic neurons and advancing the pathology. Internalized F-αSyn can be eliminated by lysosomes, proteasomes, or chaperones before it replicates inside the cell. Research has shown that F-αSyn can somehow escape from endosomes, lysosomes, and proteasomes and replicate itself. However, the impact of chaperones on intracellular levels during the initial hours of their internalization remains unknown. The present study investigates the effect of F-αSyn on chaperone levels within the first 6 and 12 h after internalization. Our findings showed that within the first 6 h, Hsc70 and Hsp90 levels were increased, while within 12 h, F-αSyn leads to a decrease or suppression of numerous intracellular chaperone levels. Exploring the pathological effects of PD on cells will contribute to identifying more targets for therapeutic interventions.

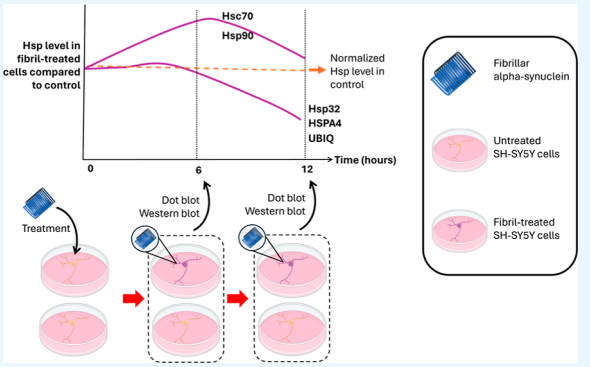

INTRODUCTION

Alpha-synuclein (αSyn) is a 140 kDa protein known as the primary component within Lewy bodies (LBs), which are pathological indicators of Parkinson's disease (PD) and dementia with LBs.[1,2] While it exists in a monomeric state under physiological conditions, its pathological forms include oligomers, protofibrils, and fibrils.[3] Fibrillar α-synucleins (F-αSyns) constitute aggregates formed by beta-sheet conformation monomers. F-αSyns have the ability to amplify themselves like disease-causing prions in vitro and in vivo.[4] It is considered that F-αSyn can spread the pathology cell-to-cell.[5] This process includes many stages, including internalization of F-αSyn, overcoming the cellular defense mechanism, amplification of F-αSyn in a prion-like manner, transportation throughout the cell, and transferring of F-αSyn to another cell.[6] However, cells have strategies to block the protein aggregation processes, such as autophagy-lysosome system, proteasomes, and chaperones.[7]

Experimental models have demonstrated that F-αSyns can localize within intracellular compartments following administration to neurons.[8] F-αSyn has the ability to somehow surpass the cellular protein quality control system, comprising lysosomes, autophagosomes, proteasomes, and chaperones.[6,9] For instance, during the initial stages of cellular internalization, F-αSyns have been observed to colocalize with early endosomes, late endosomes, and lysosomes.[8] Subsequently, they seem to escape from these membranous structures, resulting in their unrestricted presence within the cytoplasm.[6] Free F-αSyns then have the opportunity to interact with intracellular αSyns, triggering their nucleation.[10] However, other components of cellular defense, such as the ubiquitin proteasome system (UPS) and heat shock proteins (HSPs), can impede this nucleation process. Yet, given that F-αSyns inhibit the UPS in dopaminergic cells;[11] intracellular chaperones might represent the most viable remaining option.

HSPs are evolutionary conserved proteins, and they are part of the protein quality control system that also prevents protein aggregation. They are classified according to their molecular weight.[12] They participate in protein folding or refolding as well as protein degradation, stability, and transport.[13] While most of them are constitutively expressed and play roles in cells under physiological conditions, under toxic conditions such as temperature changes and infection, intracellular levels of HSPs increase to help cells survive.[14] In vitro studies have shown that, in suitable conditions, HSPs effectively disaggregate or prevent the nucleation of the fibrils.[15] Therefore, the early stages of the

Received: December 15, 2023
Revised: February 26, 2024
Accepted: February 29, 2024
Published: April 4, 2024

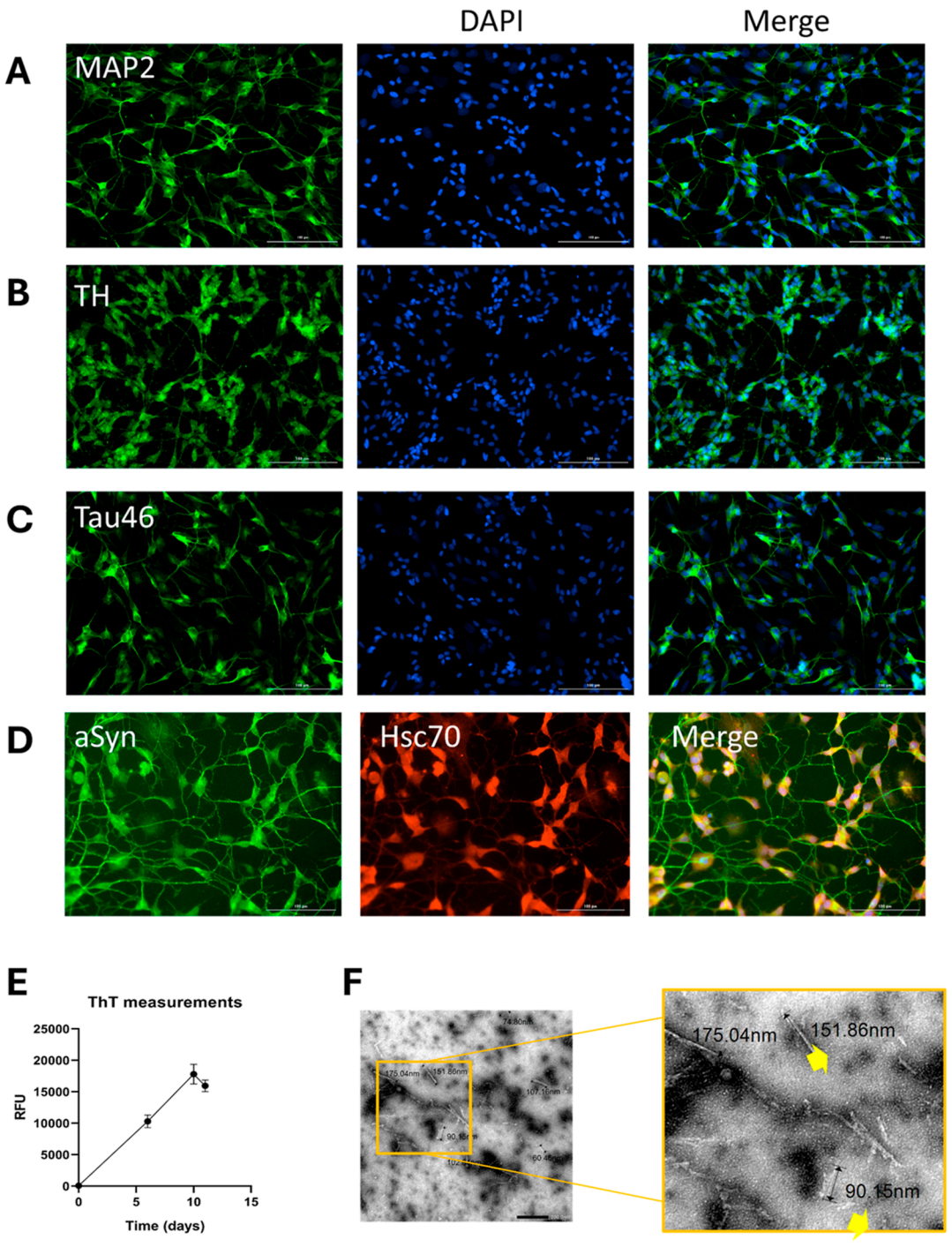

Figure 1. Neuron-like morphology and gene expression of N-SH cells and preparation of sF-αSyn. N-SH cells immunolabeled with (A) MAP2 (green) (magnification: 20×), (B) TH (green) (magnification: 20×), and (C) tau46 (green) (magnification: 20×). (D) αSyn (green) and Hsc70 (red) were double-immunolabeled (magnification: 20×). Nuclei is stained with DAPI (blue). (E) Fibrillization of αSyn was verified with ThT tests. (F) Validation of fibril fragmentation. TEM imaging was carried out after preparation of sF-αSyn. Yellow arrows show a fragment of sF-αSyn. Fragments were measured as 50−200 nm in length.

internalization of the fibrils can be critical for cell viability and to prevent nucleation before F-αSyns contact to monomeric αSyns.[16]

It was shown that in αSyn-related toxicity was reduced by overexpression of Hsp70.[17] The accumulation of misfolded proteins during cellular stress effectively triggers chaperone expression through a signaling cascade involving the transcription factor heat shock factor 1 (HSF-1).[18,19] Therefore, in this study, we investigated the intracellular HSP response of the cells to F-αSyn. We exposed cells to F-αSyn and assessed the intracellular levels of Hsp10, Hsp27, Hsp32, Hsp40, Hsp60, Hsc70, HSPA4, GRP75, Hsp90, and ubiquitin (UBIQ). In addition, fibrillar amyloid beta 1-42 (F-Aβ1-42) treatment was performed as another amyloid structured substance control.

RESULTS

Differentiated SH-SY5Y Cells Synthesize Hsc70 and Alpha-Synuclein Proteins. The neuron-like morphology of

https://doi.org/10.1021/acsomega.3c10036
ACS Omega 2024, 9, 17185−17194

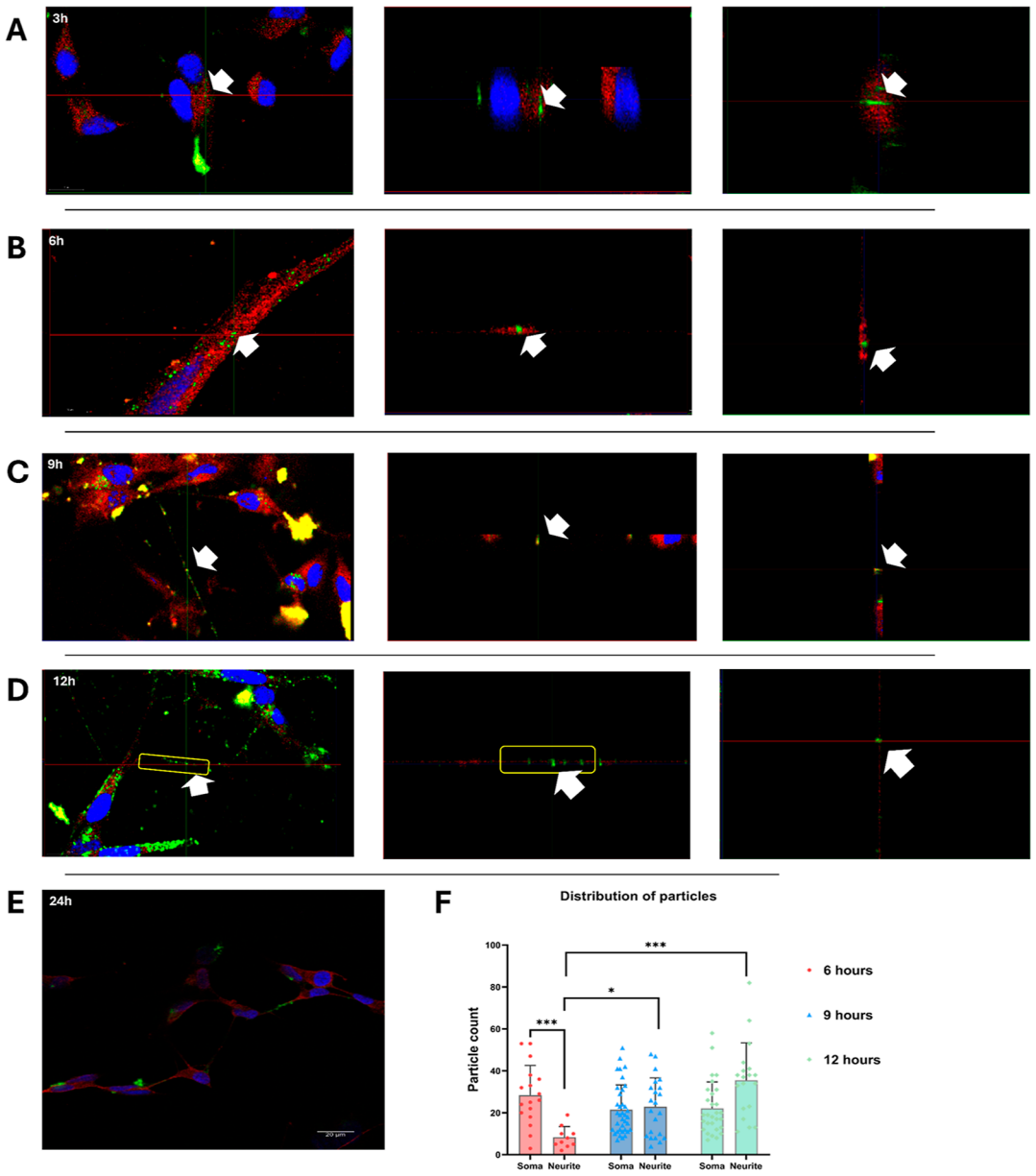

Figure 2. Validation of the F-αSyn internalization by the cells. Internalization of sF-αSyn-488 (green) was validated with confocal microscopy. (A−E) show 3, 6, 9, 12, and 24 h treatment confocal images, respectively. MAP2 (red) was immunolabeled as intracellular marker. Cells nuclei were stained with DAPI (blue) (magnification: 63×). White arrows show chosen fibrils proving they are inside the cells. Yellow square surrounds many of the fibrils inside the extensions. (F) Graphic shows distribution of internalized F-αSyn-488 particles between cell's somas and neurites in every incubation time (*: $p < 0.05$; ***: $p < 0.0008$).

differentiated SH-SY5Y (N-SH) cells was confirmed by fluorescent labeling of MAP2, TH, and tau46 (Figure 1A−C, respectively). The cells displayed long neurites and formed connections with each other. Constitutively expressed HSP, Hsc70, and αSyn were also shown in N-SH cells (Figure 1D). Both proteins colocalized, particularly in the soma region. Moreover, αSyn was especially seen in the extensions. The expression of αSyn is important for modeling cellular exposure to fibrils because extracellular sonicated F-αSyn (sF-αSyn) can amplify itself with endogenous αSyn.

Alpha-Synuclein Fibrillization and Internalization of Sonicated Fibrils. The fibrillization of αSyn was assessed and validated using the thioflavin T (ThT) test. On day 10, ThT signals reached their peak, and on day 11, the reaction was terminalized after the final measurement (Figure 1E). Then the fibrils were sonicated and analyzed with transmission electron microscopy (TEM). In TEM, sF-αSyns were measured as 50−200 nm in length (Figure 1F) and 9−14 nm in width (data not shown). Only sF-αSyns were applied to the cells.

To confirm cellular uptake, fibrils were labeled with Alexa Fluor 488 and sonicated before being applied to N-SH cells. Immunofluorescent labeling of MAP2 was used as an intracellular marker for confocal microscopy imaging. After 3 h of treatment, analysis showed that the cells had internalized sF-αSyn (Figure 2A). By 6 h, sF-αSyn was predominantly localized inside the cells (Figure 2B). sF-αSyn was observed in cellular extensions, particularly at the 9 and 12 h marks (Figure 2C,D, respectively). After 24 h, the intensity of the fluorescent signal from the labeled sF-αSyn decreased (Figure 2E).

https://doi.org/10.1021/acsomega.3c10036
ACS Omega 2024, 9, 17185−17194

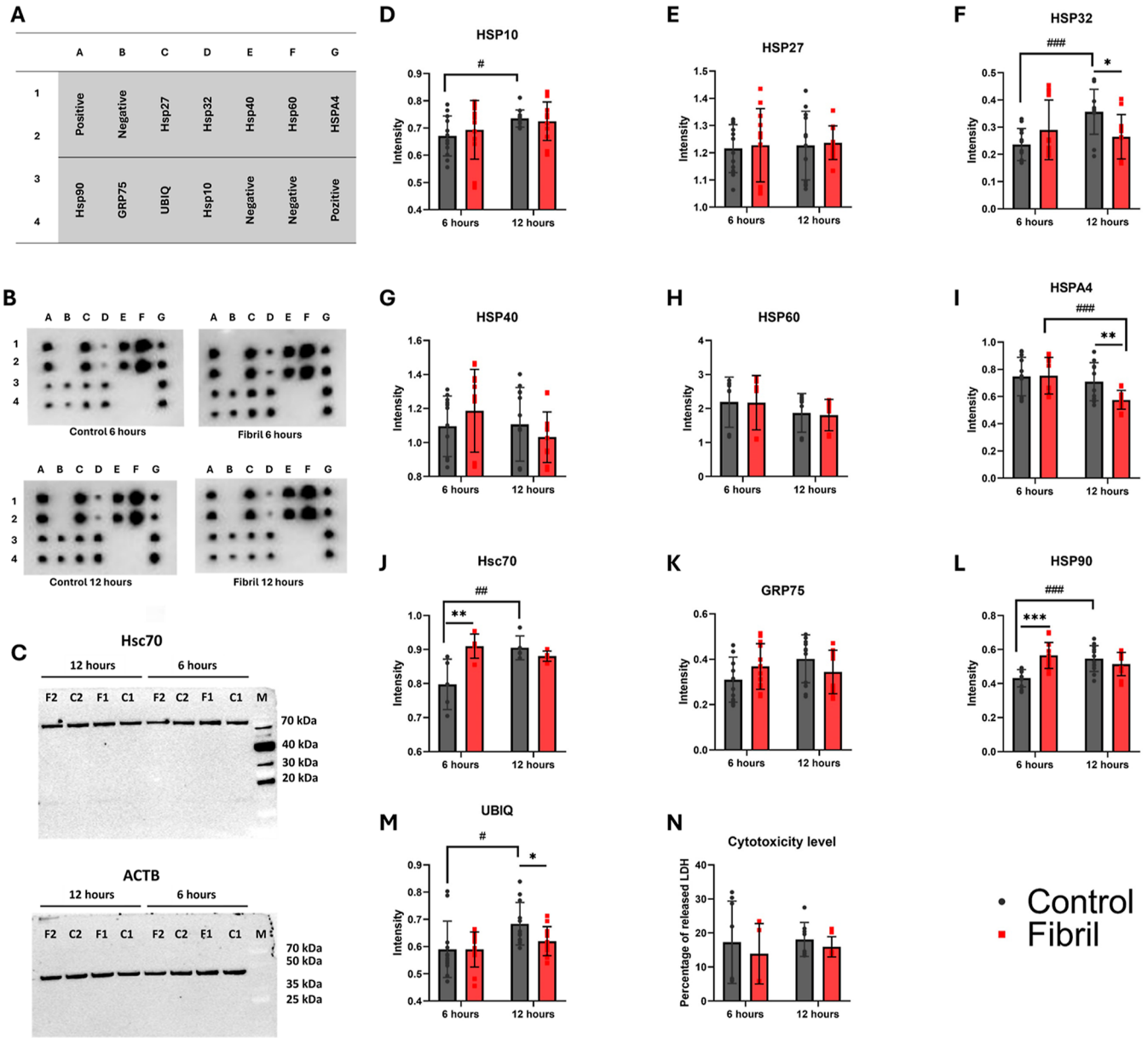

Figure 3. DB and WB membranes and graphics show total cellular expression levels of the Hsps. (A) Localization map of the chaperone-specific antibodies on the DB membranes. (B) Images of the DB membranes of 6 and 12 h control and treatment groups. (C) WB membrane of Hsc70 and ACTB (M: marker; C1, C2: control group samples of repeated experiments; and F1, F2: fibril group samples of repeated experiments.). (D−M) Graphics showing the intracellular level changes of Hsp10, Hsp27, Hsp32, Hsp40, Hsp60, HSPA4, Hsc70, GRP75, Hsp90, and UBIQ. (N) Percentages of cytotoxicity based on released LDH level ("*" was used on the graphs to show statistical significance between groups in same time point; "#" was used on the graphs to show statistical significance inside the experimental groups over time. * and #: $p < 0.05$; ** and ##: $p < 0.01$; *** and ###: $p < 0.001$).

The distribution of internalized F-αSyn-488 between cell somas and neurites over time was assessed from confocal images. Due to the insufficient amount at 3 and 24 h, the analysis was conducted at 6, 9, and 12 h. At 6 h, F-αSyn-488 predominantly localized in the cell soma region ($p = 0.0007$). Over time, the distribution of labeled fibrils increased in cellular neurites at 9 h compared to neurites at 6 h ($p < 0.03$). By 12 h, neuritic F-αSyn-488 content reached its peak, surpassing the content at 6 h ($p < 0.0001$) (Figure 2F).

Based on these results, we investigated the possible changes in intracellular chaperone levels at the 6 h time point since most fibrils entered the cells first within this time frame. However, the observation of fibrils in the cellular extensions led us to consider that the cells could process the fibrils, which may be free in the cytoplasm, and undergo initial chaperone interventions. Therefore, we selected the 6 and 12 h time intervals to determine intracellular chaperone levels.

Chaperone Profile in Response to sF-αSyn. The results obtained from confocal microscopy were used as a guide to analyze the time intervals of chaperone expression. Accordingly, we investigated the chaperone response of cells to sF-αSyn during the first 6 h, when sF-αSyn-488 was found to be dominantly inside the cells, and during the subsequent 6 h, when it was observed in cellular extensions. Therefore, N-SH cells were incubated with sF-αSyn for 6 and 12 h, and then early chaperone level profiles were analyzed. Untreated N-SH cells

https://doi.org/10.1021/acsomega.3c10036
ACS Omega 2024, 9, 17185−17194

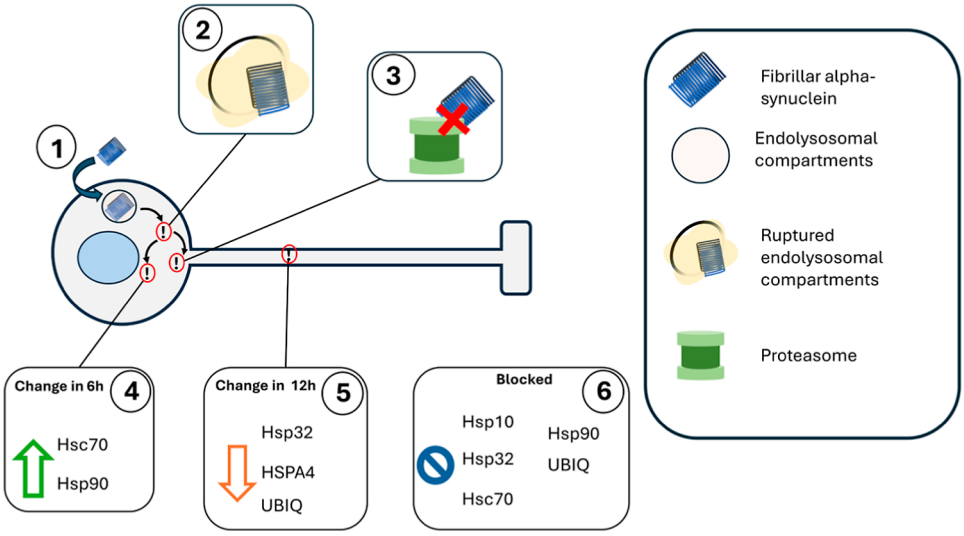

Figure 4. Comparison of our findings with previous findings in the literature. Studies have shown that F-αSyns internalized by the cells and generally localized in endosomes or lysosomes (1). Fibrils somehow released from these membranous structures and became free in the cytoplasm (2). Proteasome machinery does not efficiently degrade F-αSyn (3). In addition to these findings, our study provides information about the situation of another protein quality control unit, chaperones, in the early stages. In the first 6 h, Hsc70 and Hsp90 significantly respond by increasing (4). However, after 6 h, Hsp32, HSPA4, and UBIQ levels decrease (5). Finally, our study has also shown that F-αSyn blocks Hsp10, Hsp32, Hsc70, Hsp90, and UBIQ to increase, based on the comparison the group's change over time (6).

with the same time intervals were used as controls. Total protein isolations were performed from cells 6 and 12 h.

Total protein samples were analyzed to determine the intracellular levels of chaperones using both dot blot (DB) and western blot (WB) techniques. Each DB membrane contained 9 chaperones: Hsp27, Hsp32, Hsp40, Hsp60, HSPA4, Hsp90, GRP75, UBIQ, and Hsp10 (Figure 3A). DB membranes are presented in Figure 3B. The expression level of Hsc70 was determined by WB, and beta-actin (ACTB) served as the housekeeping control, imaged on the same membrane (Figure 3C). The data were analyzed in two ways: evaluating the significance of the differences between the control and treated cells within the same time interval and assessing the significance of time-dependent changes through intragroup assessment.

The overall results show that intracellular levels of Hsp27, HSP40, Hsp60, and GRP75 did not exhibit statistically significant changes ($p > 0.05$) (Figure 3E,G,H,K, respectively). On the other hand, after 6 h of incubation with sF-αSyn, there were no significant differences in the levels of chaperones except for Hsc70 and HSP90, which showed increased levels compared to the untreated control (Figure 3J,L, respectively) ($p = 0.006$ and $p < 0.0001$, respectively). However, after 12 h of treatment with sF-αSyn, the levels of HSP32, HSPA4, and UBIQ decreased compared to the control (Figure 3F,I,M, respectively) ($p = 0.01$, $p = 0.009$, and $p < 0.03$, respectively).

On the other hand, when considering the intragroup changes over time, significant alterations were observed in many chaperones. The levels of HSP10, HSP32, Hsc70, HSP90, and UBIQ (Figure 3D,F,J,L,M, respectively) were 0.01, 0.0004, 0.008, and 0.0002, and $p = 0.02$, respectively. Moreover, the level of HSPA4 decreased with 12 h of sF-αSyn treatment compared to 6 h of treatment (Figure 3I) ($p = 0.0009$).

Chaperone expression profile was different in 6 and 12 h of 1 μM F-Aβ1-42 treatment (Figure S1). Additionally, the cytotoxicity assay based on secreted lactate dehydrogenase (LDH) levels did not show statistically significant changes between groups ($p > 0.05$) (Figure 3N).

DISCUSSION

In recent years, monoclonal antibody-based treatments have received conditional approval for Alzheimer's disease (AD).[20] Unfortunately, monoclonal antibody therapies tested for PD have not yielded the desired outcomes.[21] The reason for this might be the ability of F-αSyn, acting like a prion, to replicate itself within the cell and evade extracellular interventions. The early internalization process could provide crucial targets for preventing the propagation of PD pathology. For instance, strengthening lysosomes, which are barriers overcome by fibrils during early internalization, has been demonstrated to enhance cellular defense capacity against the pathology.[22] Moreover, the inhibition of the autophagy-lysosomal pathway resulted in an increased release of αSyn.[23] On the other hand, when F-αSyns are released from endosomal-lysosomal structures, and because they can disrupt UPS,[11] cytoplasmic chaperones become the most robust cellular defense system against them. Therefore, targeting intracellular pathological pathways for the treatment of PD might yield promising results. However, intervening within the cell could lead to undesired consequences because of the possible disruption of normal cellular functions. Hence, identifying multiple distinct targets, in this case, different chaperones, for inhibiting F-αSyn propagation would increase the pathway diversity. Given that, this study investigates how chaperones respond during the initial hours of F-αSyn internalization. Our findings, along with a comparison to the literature, are summarized in Figure 4.

It has been expressed that αSyn aggregates somehow overcome the endosomal and lysosomal pathways.[6] While αSyn aggregates can be degraded in lysosomes, F-αSyn can escape from endolysosomal complexes by disrupting or rupturing their membranes, following internalization by the cells.[24,25] Once escaped, free F-αSyn in the cytoplasm can access the monomers necessary for self-amplification, initiating the process that leads to LB formation within the cell.[10,26,27] However, the protein quality control system also includes other components, such as the UPS and chaperones, which can

https://doi.org/10.1021/acsomega.3c10036
ACS Omega 2024, 9, 17185−17194

effectively manage F-αSyn.[28] Although the chaperone activity is not expression-dependent, it is known that an elevated quantity of chaperones is one of the cellular protective mechanisms under certain conditions to for cells to survive.[14] Therefore, initially, we hypothesized that fibrils might have toxic effects on cells, potentially leading to an increase in chaperone levels. However, our findings revealed no increase in expression except for Hsc70 and Hsp90; conversely, a decrease was observed after 12 h fibril treatment. Additionally, we found that these findings are specific to F-αSyn, as the cellular response to F-Aβ1-42 differs from that of F-αSyn under similar experimental conditions. The decrease in response to F-αSyn treatment in the levels of Hsps could render cells vulnerable in several ways. First, it could weaken cellular protein functions due to the reduced levels of chaperones necessary for normal cellular processes, while simultaneously increasing chaperone levels, which might benefit the fibrils themselves. Second, fibrils might gain more time to interact with monomeric forms acting as substrates and potentially replicate themselves.

However, expression levels of Hsp27, Hsp40, Hsp60, and GRP75 have not shown any changes. In previous post-mortem studies, increased Hsp27 expression has been demonstrated in samples taken from the cortex of Parkinson's patients.[29] This suggests that prolonged exposure to proliferating F-αSyns as the disease progresses might enhance chaperone expression. On the other hand, Hsp40 is a class of chaperones that regulate Hsp70 chaperones by acting as cochaperone by stimulating ATP hydrolysis.[30] Studies have demonstrated that in the presence of Hsp100, ATP, and Hsp40, Hsc70 can facilitate the degradation of F-αSyns.[31] The maintenance of Hsp40 levels and the increase in Hsc70 levels support the resistance of cells to fibrillar forms. On the other hand, in the context of neurodegeneration, it has been demonstrated that Hsc70 contributes to the release of proteins associated with neurodegeneration, such as αSyn and tau.[32] Consequently, an increase in Hsc70 levels may facilitate their cell-to-cell spreading.

However, Hsc70 is a constitutively expressed chaperone, and the intracellular levels of HSPA4, which is the HSP induced by toxicity, have decreased in our findings. This could potentially weaken interventions against toxicity. Additionally, the lack of significant changes in the levels of LDH released into the culture supernatant could be attributed to the relatively low toxic effect on cells. This situation may explain the lack of an increase in HSPA4 expression.

The interaction of αSyn with mitochondria may occur not only through mitochondrial deoxyribonucleic acid, as previously predicted,[33] but also through mitochondrial chaperones GRP75 is a mitochondria-associated membrane chaperone essential for regulating mitochondrial turnover and involved in energy production processes,[34,35] we did not find any significant change at the intracellular level of this chaperone. Conversely, another mitochondrial chaperone, Hsp10, displayed an increase in levels within the first 12 h in the control group, a response not observed in the presence of fibrils. We interpret this as the suppression of this chaperone. The weakening of HSP10 may represent another significant factor contributing to the decline in mitochondrial function during the progression of PD. Studies have demonstrated a correlation between the knockdown of this chaperone and the occurrence of hypometabolism and oxidative stress.[36] This suggests that under chronic exposure to F-αSyns, the essential energy required for the survival of substantia nigra dopaminergic neurons, lacking myelin and having high energy demands, may not be adequately supplied. Consequently, this could lead to a detrimental effect on these neurons compared with the impact of the PD process alone.

On the other hand, the increase in the presence of Hsp90 after 6 h may render the chaperone system vulnerable. Hsp90 is known for its role in stabilizing proteins,[37] and it can exhibit this property for F-αSyn as well. F-αSyn can use Hsp90 as a facilitator during the early internalization stages by increasing its levels, which in turn can stabilize protein aggregates.[38] Therefore, at this stage, Hsp90 can potentially work in favor of fibrils. Additionally, Hsp90 exerts control over the expression of other HSPs by regulating HSF-1. In its inactive monomeric state, HSF-1 is primarily located in the cytoplasm and is maintained by Hsp90.[39] Hence, the increased level of Hsp90 at the 6 h mark may be linked to the decreased levels of other HSPs observed at 12 h. This idea gains support from previous research indicating the beneficial effects of inhibiting Hsp90 by small inhibitors.[40] Nevertheless, Hsp90 level was found to be reduced in early and late-onset AD.[41] In our study, the Hsp90 level did not change significantly after 12 h of treatment compared to the control group. However, its levels may decrease with chronic exposure to the fibrils. Furthermore, the reduction in the amount of UBIQ could potentially have a diminishing effect on protein degradation, thereby supporting the replication of F-αSyn. This process bears similarities to viral infections, where certain viruses can reduce UBIQ levels upon entering cells.[42]

Finally, alterations in the levels of chaperones were primarily observed after 12 h of incubation, potentially resulting from reduced expression levels or enhanced degradation of them. On the other hand, this study primarily focused on the initial hours of fibril infection, and longer incubation periods could potentially affect the levels of other chaperones such as Hsp27, Hsp40, Hsp60, and GRP75. However, further research is needed to confirm these assumptions.

MATERIALS AND METHODS

Alpha-Synuclein Fibrillization. αSyn fibrillization carried out as previously described.[43] Briefly, recombinant αSyn (Millipore, AG938-1MG) was dissolved in phosphate-buffered saline (PBS) in 140 μM concentration and incubated 37 °C at 400 rpm. The reaction was followed by a ThT test. For this, in the final concentration, 4.5 μM peptide was taken from the reaction sample, and 20 μM ThT was mixed in PBS and incubated for 1 h at 37 °C and 400 rpm. Measurements were taken with a Biotek SynergyHT spectrofluorometer with 440 excitation and 485 emission filter set. The reaction was terminated when ThT measurements made a plateau on day 11. The fibril-containing sample was centrifuged at 20,000*g* for 30 min. The supernatant was discarded, and the pellet was washed with PBS and centrifuged. The washing was repeated twice. Amyloid beta 1−42 (Aβ1-42) fibrillization was performed as described previously.[44] Briefly, the Aβ1-42 (Millipore, AG938-1MG) was reconstituted in PBS and incubated at 1000 rpm for 24 h at 37 °C.

The fluorescent labeling of the αSyn fibrils was performed according to the manufacturer's instruction. Shortly, 2 mg/mL fibrils were dissolved in 0.1 M sodium bicarbonate buffer (pH 8.3) and incubated with Alexa Fluor 488 dye (Thermo Fisher, A20000) in a 1:2 protein: dye ratio at room temperature for 1 h. The reaction sample was washed three times to remove any unbounded dyes. Before applying to the cells, fibrils were fragmented by an ultrasonicator (QSonica, Q800R3) with pulses of 3 sn on/2 sn off and 30% amplitude for 15 min at 15 °C, as described before.[45]

https://doi.org/10.1021/acsomega.3c10036
ACS Omega 2024, 9, 17185−17194

sF-αSyn was analyzed by TEM to show the success of the sonicated fibril preparation. For TEM analysis, a 10 μL sample was deposited on a Formvar/carbon-coated 200-mesh copper grid (Ted Pella, Inc.). Without letting the grids dry, they were stained with 20 μL of a 2% uranyl acetate alternative solution and then air-dried at room temperature. Grids were imaged by using a JEOL JEM-2100PLUS electron microscope equipped with a LaB6 source operated at 200 kV.

Cell Culture and Fibril Application. SH-SY5Y cells were seeded and differentiated in a 1:50 poly-L-ornithine (Sigma-Aldrich, P4957)-coated Petri dishes as described before.[46] Before differentiation, the cells were cultured in basal media containing MEM (Thermo Fisher, 31095-029):F12 (Thermo Fisher, 21765-029) (1:1), 10% FBS (Thermo Fisher, 10270106), 1% nonessential amino acid solution (Thermo Fisher, 11140-050), and 1 mM sodium pyruvate (Sigma-Aldrich, P2256-100G). The cells passaged at 90% confluency and differentiated into neurons by neurobasal media (Gibco, 12348017) supplemented with 1× B27 (Gibco, 17504-044), 0.063% NaCl, 1× L-glutamine (Gibco, 25030-024), 0.1 mM putrescine (Sigma, P7505), 10 ng/mL insulin (Gibco, 12585-014), 20 μM progesteron (Sigma, P6149), 0.25% conalbumin (Sigma-Aldrich, C7786), 1% FBS (Thermo Fisher, 10270106), 10 μM retinoic acid (Sigma, R2625), and 50 ng/mL BDNF (Sigma, b3795) when the confluency reached 40%. The cells were cultured in differentiation media for at least 8 days, and the media was changed every 3−4 days. Differentiation was validated with morphological changes and fluorescent labeling.

To determine whether the fibrils were internalized, they were sonicated, and Alexa Fluor 488-labeled 1 μM F-αSyn (sF-αSyn-488) was applied to the cells as described previously[47] and incubated for 3, 6, 9, 12, and 24 h. At the end of the incubation, the cells were washed 3 times with PBS and then fixed with 3.7% PFA. MAP2 was immunolabeled and analyzed with confocal microscopy.

For the analysis of chaperone levels, protein isolation was performed after 6 and 12 h of incubation. Briefly, on the seventh day of differentiation, 1 μM sF-αSyn or 1 μM F-Aβ1-42 applied to the cells, and total protein isolation was performed with M-PER (Thermo Fisher, 78501), including 1× PhosStop (Roche, 4906845001) and a 10% Halt protease inhibitor (Thermo Fisher, 1861280). Proteins were immediately stored at −80 °C until the use.

Immunofluorescent Labeling and Analysis. The cells were seeded and differentiated on coverslips. To validate differentiation with immunofluorescent labeling, the cells were cultured and differentiated on coverslips, then fixed with 3 and 7% PFA for 15 min at RT. The fixed cells were permeabilized and blocked at room temperature for 1 h with 0.02% TPBS containing 30% BSA. The primary antibodies, which are anti-MAP2 (Thermo Fisher, MA5-12826) (1/250), antityrosine hydroxylase (TH) (Thermo Fisher, 701949) (1/75), and antitau (Thermo Fisher, 136400) (1/150), in 0.02% TPBS containing 1.5% BSA, were applied to the coverslips overnight at 4 °C. The secondary antibodies conjugated with Alexa Fluor 488 (Thermo Fisher, A11034 or Abcam, ab150117) (1/200) were applied and incubated at room temperature for 1 h.

Hsc70 and αSyn expression were validated with double immunofluorescent labeling. Anti-Hsc70 antibody (Novusbio, NBP2-67335) (1/200) was applied to the coverslips overnight, followed by a secondary antibody (Thermo Fisher, A32740) application. After three times washing, anti-αSyn antibody (Thermo Fisher, 328100) (1/200) was applied, and coverslips were incubated at room temperature for 2 h, followed by secondary antibody (Abcam, ab150117) application and incubation at RT for 1 h. The cell nuclei were stained with 4′,6-diamidino-2-phenylindole (DAPI). The coverslips were mounted using a Biotek Lionheart FX live cell imaging system.

For fibril uptake analysis, sF-αSyn-488 was applied to differentiated cells on coverslips, and the cells were incubated for 3, 6, 9, 12, and 24 h and then fixated. The fixation was followed by immunofluorescent labeling of MAP2 (Thermo Fisher, MA5-12826) (1/250) and secondary antibody application targeting anti-MAP2 antibody (Thermo Fisher, A32740). The coverslips were analyzed with a Leica TCS SP8 confocal microscope using LasX software.

The distribution of internalized F-αSyn-488 between cell somas and neurites over the incubation times was determined in confocal images by using ImageJ software. In brief, the images were processed separately in ImageJ, and threshold adjustments were performed for each image to maximize the detection of the particles. The adjusted images were then converted to binary, and the "convert to mask" function was applied. Subsequently, soma or neurite regions of the cells were selected, and particle analysis in the "analyze" tab was performed. With this function, ImageJ provides various properties of the particles, including the counts of particles in the selected region. This process was performed for every cell in the images.

Western Blot and Dot Blot. For WB, the proteins were thawed, and concentrations were measured with a nanodrop one (Thermo Fisher). Proteins were normalized to 40 μg per well and mixed with a 4× sample buffer (Thermo Fisher, B0007) containing 10% beta-mercaptoethanol. The samples were boiled at 100 °C for 5 min before being loaded to the wells. After electrophoresis, the proteins were transferred to poly(vinylidene difluoride) membranes (Thermo Fisher, PB5310) with a Trans-Blot Turbo transfer system (Biorad, 1,704,150). The membranes were blocked with 5% skim milk for 1 h at RT and incubated overnight at 4 °C with anti-HSC70 antibody (Novusbio, NBP2-67335) (1/750) and antiactin beta antibody (Abcam, ab8226) (1/3000), followed by 2 h incubation at RT with antirabbit IgG (Invitrogen, 65-6120) (1/3000) or antimouse IgG secondary antibodies (Abcam, ab97040) (1/3000). Membranes were treated with chemiluminescent substrate (Thermo Fisher, 34580), and the signals were taken with a Biorad ChemiDoc imager.

DB experiments were performed using HSP DB kit (RayBiotech, AAH-HSP-1-8) as previously described.[48] Briefly, the samples were normalized to 230 μg, mixed with blocking buffer, and loaded to preblocked membranes. The membranes were incubated overnight at 4 °C and washed, and a HSP antibody mixture was applied. The membranes were incubated overnight at 4 °C. The next day, they were washed, and streptavidin solution was applied. After incubation for 2 h at RT, chemiluminescent substrate was applied to the membranes, and images were taken with the Biorad ChemiDoc imager. Band intensities were quantified with ImageJ software.

LDH Cytotoxicity Test. Cytotoxicity was determined as previously described[49] with the secreted LDH level in the culture media. Each sample was measured according to the manufacturer's instructions (Roche, 11644793001) in triplicate with the BioTek SynergyHT instrument. The percentage of the released LDH levels was calculated as described in the kit's protocol.

Statistical Analysis. DB dot's and WB band intensities were measured using ImageJ software. For DB, measurements were

https://doi.org/10.1021/acsomega.3c10036
ACS Omega 2024, 9, 17185−17194

processed in the RayBio Analysis Tool for AAH-HSP-1-8 before statistical analysis of the levels of Hsp27, Hsp32, Hsp40, Hsp60, HSPA4, Hsp90, GRP75, UBIQ, and HSP10. For the analysis of the distribution of internalized F-αSyn-488 between soma and neurites, the counted particles in confocal images were compared within the same time interval and between the same cell region at different time intervals. The values were compared by GraphPad Prism 8 software (GraphPad Software, Inc., San Diego, USA). The comparisons were performed according to whether the values were distributed normally, and whether the difference between the SDs was significant. This is carried out first by a one-way analysis of variance, followed by Tukey Kramer multiple comparison tests or first by Kruskal–Wallis, and then with Dunn's multiple comparison tests.

■ ASSOCIATED CONTENT

Data Availability Statement

All the data generated or analyzed in this study are presented in this published article.

Supporting Information

The Supporting Information is available free of charge at https://pubs.acs.org/doi/10.1021/acsomega.3c10036.

Short-term (6 and 12 h) chaperone expression profile analysis in cells treated with 1 μM F-Aβ1-42 (PDF)

■ AUTHOR INFORMATION

Corresponding Author

Duygu Gezen-Ak − *Brain and Neurodegenerative Disorders Research Laboratories, Department of Neuroscience, Institute of Neurological Sciences, Istanbul University-Cerrahpasa, Istanbul 34098, Turkey;* orcid.org/0000-0001-7611-2111; Phone: +90 212 414 30 00/22032; Email: duygugezenak@iuc.edu.tr

Authors

Tugay Çamoğlu − *Brain and Neurodegenerative Disorders Research Laboratories, Department of Neuroscience, Institute of Neurological Sciences, Istanbul University-Cerrahpasa, Istanbul 34098, Turkey*

Zuhal Yurttaş − *Brain and Neurodegenerative Disorders Research Laboratories, Department of Neuroscience, Institute of Neurological Sciences, Istanbul University-Cerrahpasa, Istanbul 34098, Turkey*

Ümit Yaşar Kına − *Beykoz Institute of Life Sciences and Biotechnology, Bezmialem Vakif University, Istanbul 34093, Turkey;* orcid.org/0000-0003-2872-533X

Pınar Akkuş Süt − *Department of Genetics and Bioengineering, Faculty of Engineering, Yeditepe University, Istanbul 34755, Turkey*

Fikrettin Sahin − *Department of Genetics and Bioengineering, Faculty of Engineering, Yeditepe University, Istanbul 34755, Turkey*

Erdinç Dursun − *Brain and Neurodegenerative Disorders Research Laboratories, Department of Neuroscience, Institute of Neurological Sciences, Istanbul University-Cerrahpasa, Istanbul 34098, Turkey;* orcid.org/0000-0003-3701-6674

Complete contact information is available at: https://pubs.acs.org/10.1021/acsomega.3c10036

Author Contributions

Conceptualization, T.Ç. and D.G.-A.; methodology, T.Ç., Z.Y., E.D., and D.G.-A.; software, T.Ç. and D.G.-A.; validation, T.Ç. and D.G.-A.; formal analysis, T.Ç. and D.G.-A.; investigation, T.Ç., Z.Y., E.D., and D.G.-A.; resources, T.Ç., Z.Y., and D.G.-A.; data curation, T.Ç., Z.Y., E.D., Ü.Y.K., P.A.S., F.S., and D.G.-A.; writing−original draft preparation, T.Ç., Z.Y., E.D., and D.G.-A.; writing−review and editing, T.Ç., Z.Y., E.D., and D.G.-A.; visualization, T.Ç., Z.Y., and D.G.-A.; supervision, D.G.-A.; project administration, D.G.-A.; and funding acquisition, D.G.-A. All authors have read and agreed to the published version of the manuscript.

Notes

The authors declare no competing financial interest.

■ ACKNOWLEDGMENTS

This study is supported by the Istanbul University-Cerrahpasa Scientific Research Project Unit (project ID: 33479). The funders had no role in study design, data collection and analysis, the decision to publish, or the preparation of the manuscript.

■ REFERENCES

(1) Bendor, J. T.; Logan, T. P.; Edwards, R. H. The function of α-synuclein. *Neuron* **2013**, *79* (6), 1044−1066.

(2) Spillantini, M. G.; Crowther, R. A.; Jakes, R.; Hasegawa, M.; Goedert, M. α-Synuclein in filamentous inclusions of Lewy bodies from Parkinson's disease and dementia with Lewy bodies. *Proc. Natl. Acad. Sci. U.S.A.* **1998**, *95* (11), 6469−6473.

(3) Cremades, N.; Dobson, C. M. The contribution of biophysical and structural studies of protein self-assembly to the design of therapeutic strategies for amyloid diseases. *Neurobiol. Dis.* **2018**, *109*, 178−190.

(4) Olanow, C. W.; Brundin, P. Parkinson's Disease and Alpha Synuclein: Is Parkinson's Disease a Prion-Like Disorder? *Mov. Disord.* **2013**, *28* (1), 31−40.

(5) Kim, S.; Kwon, S.-H.; Kam, T.-I.; Panicker, N.; Karuppagounder, S. S.; Lee, S.; Lee, J. H.; Kim, W. R.; Kook, M.; Foss, C. A.; Shen, C.; Lee, H.; Kulkarni, S.; Pasricha, P. J.; Lee, G.; Pomper, M. G.; Dawson, V. L.; Dawson, T. M.; Ko, H. S. Transneuronal Propagation of Pathologic α-Synuclein from the Gut to the Brain Models Parkinson's Disease. *Neuron* **2019**, *103* (4), 627−641.e7.

(6) Bieri, G.; Gitler, A. D.; Brahic, M. Internalization, axonal transport and release of fibrillar forms of alpha-synuclein. *Neurobiol. Dis.* **2018**, *109*, 219−225.

(7) Ciechanover, A.; Kwon, Y. T. Protein quality control by molecular chaperones in neurodegeneration. *Front. Neurosci.* **2017**, *11*, 1−18.

(8) Konno, M.; Hasegawa, T.; Baba, T.; Miura, E.; Sugeno, N.; Kikuchi, A.; Fiesel, F. C.; Sasaki, T.; Aoki, M.; Itoyama, Y.; Takeda, A. Suppression of dynamin GTPase decreases α-synuclein uptake by neuronal and oligodendroglial cells: A potent therapeutic target for synucleinopathy. *Mol. Neurodegener.* **2012**, *7* (1), 38.

(9) Saibil, H. Chaperone machines for protein folding, unfolding and disaggregation. *Nat. Rev. Mol. Cell Biol.* **2013**, *14* (10), 630−642.

(10) Aulić, S.; Le, T. T. N.; Moda, F.; Abounit, S.; Corvaglia, S.; Casalis, L.; Gustincich, S.; Zurzolo, C.; Tagliavini, F.; Legname, G. Defined α-synuclein prion-like molecular assemblies spreading in cell culture. *BMC Neurosci.* **2014**, *15*, 69.

(11) Zondler, L.; Kostka, M.; Garidel, P.; Heinzelmann, U.; Hengerer, B.; Mayer, B.; Weishaupt, J. H.; Gillardon, F.; Danzer, K. M. Proteasome impairment by α-synuclein. *PLoS One* **2017**, *12* (9), No. e0184040.

(12) Tukaj, S. Heat Shock Protein 70 as a Double Agent Acting Inside and Outside the Cell: Insights into Autoimmunity. *Int. J. Mol. Sci.* **2020**, *21* (15), 5298.

(13) Gorenberg, E. L.; Chandra, S. S. The role of co-chaperones in synaptic proteostasis and neurodegenerative disease. *Front. Neurosci.* **2017**, *11*, 248.

(14) Miller, D. J.; Fort, P. E. Heat Shock Proteins Regulatory Role in Neurodevelopment. *Front. Neurosci.* **2018**, *12*, 821.
(15) Waudby, C. A.; Knowles, T. P. J.; Devlin, G. L.; Skepper, J. N.; Ecroyd, H.; Carver, J. A.; Welland, M. E.; Christodoulou, J.; Dobson, C. M.; Meehan, S. The interaction of αB-Crystallin with mature α-synuclein amyloid fibrils inhibits their elongation. *Biophys. J.* **2010**, *98* (5), 843−851.
(16) Cox, D.; Whiten, D. R.; Brown, J. W. P.; Horrocks, M. H.; San Gil, R.; Dobson, C. M.; Klenerman, D.; Van Oijen, A. M.; Ecroyd, H. The small heat shock protein Hsp27 binds α-synuclein fibrils, preventing elongation and cytotoxicity. *J. Biol. Chem.* **2018**, *293* (12), 4486−4497.
(17) Yu, W.-W.; Cao, S.-N.; Zang, C.-X.; Wang, L.; Yang, H.-Y.; Bao, X.-Q.; Zhang, D. Heat shock protein 70 suppresses neuroinflammation induced by α-synuclein in astrocytes. *Mol. Cell. Neurosci.* **2018**, *86*, 58−64.
(18) Masser, A. E.; Kang, W.; Roy, J.; Mohanakrishnan Kaimal, J.; Quintana-Cordero, J.; Friedländer, M. R.; Andréasson, C. Cytoplasmic protein misfolding titrates Hsp70 to activate nuclear Hsf1. *Elife* **2019**, *8*, No. e47791.
(19) Masser, A. E.; Ciccarelli, M.; Andréasson, C. Hsf1 on a leash—controlling the heat shock response by chaperone titration. *Exp. Cell Res.* **2020**, *396* (1), 112246.
(20) Cummings, J. Anti-Amyloid Monoclonal Antibodies are Transformative Treatments that Redefine Alzheimer's Disease Therapeutics. *Drugs* **2023**, *83* (7), 569−576.
(21) Whone, A. Monoclonal Antibody Therapy in Parkinson's Disease—The End? *N. Engl. J. Med.* **2022**, *387* (5), 466−467.
(22) Wie, J.; Liu, Z.; Song, H.; Tropea, T. F.; Yang, L.; Wang, H.; Liang, Y.; Cang, C.; Aranda, K.; Lohmann, J.; Yang, J.; Lu, B.; Chen-Plotkin, A. S.; Luk, K. C.; Ren, D. A growth-factor-activated lysosomal K+ channel regulates Parkinson's pathology. *Nature* **2021**, *591* (7850), 431−437.
(23) Minakaki, G.; Menges, S.; Kittel, A.; Emmanouilidou, E.; Schaeffner, I.; Barkovits, K.; Bergmann, A.; Rockenstein, E.; Adame, A.; Marxreiter, F.; Mollenhauer, B.; Galasko, D.; Buzás, E. I.; Schlötzer-Schrehardt, U.; Marcus, K.; Xiang, W.; Lie, D. C.; Vekrellis, K.; Masliah, E.; Winkler, J.; Klucken, J. Autophagy inhibition promotes SNCA/alpha-synuclein release and transfer via extracellular vesicles with a hybrid autophagosome-exosome-like phenotype. *Autophagy* **2018**, *14* (1), 98−119.
(24) Dilsizoglu Senol, A.; Samarani, M.; Syan, S.; Guardia, C. M.; Nonaka, T.; Liv, N.; Latour-Lambert, P.; Hasegawa, M.; Klumperman, J.; Bonifacino, J. S.; Zurzolo, C. α-Synuclein fibrils subvert lysosome structure and function for the propagation of protein misfolding between cells through tunneling nanotubes. *PLOS Biol.* **2021**, *19* (7), No. e3001287.
(25) Jiang, P.; Gan, M.; Yen, S.-H.; McLean, P. J.; Dickson, D. W. Impaired endo-lysosomal membrane integrity accelerates the seeding progression of α-synuclein aggregates. *Sci. Rep.* **2017**, *7* (1), 7690.
(26) Volpicelli-Daley, L. A.; Luk, K. C.; Patel, T. P.; Tanik, S. A.; Riddle, D. M.; Stieber, A.; Meaney, D. F.; Trojanowski, J. Q.; Lee, V. M.-Y. Exogenous α-Synuclein Fibrils Induce Lewy Body Pathology Leading to Synaptic Dysfunction and Neuron Death. *Neuron* **2011**, *72* (1), 57−71.
(27) Masuda-Suzukake, M.; Nonaka, T.; Hosokawa, M.; Oikawa, T.; Arai, T.; Akiyama, H.; Mann, D. M. A.; Hasegawa, M. Prion-like spreading of pathological α-synuclein in brain. *Brain* **2013**, *136* (4), 1128−1138.
(28) Chen, B.; Retzlaff, M.; Roos, T.; Frydman, J. Cellular Strategies of Protein Quality Control. *Cold Spring Harbor Perspect. Biol.* **2011**, *3* (8), a004374.
(29) Plath, P. Zentrale Hör- und Wahrnehmungsstörungen [Central hearing and perceptual disorders]. *HNO* **1994**, *42* (10), 600−601.
(30) Zarouchlioti, C.; Parfitt, D. A.; Li, W.; Gittings, L. M.; Cheetham, M. E. DNAJ Proteins in neurodegeneration: essential and protective factors. *Philos. Trans. R. Soc. B Biol. Sci.* **2018**, *373* (1738), 20160534.
(31) Gao, X.; Carroni, M.; Nussbaum-Krammer, C.; Mogk, A.; Nillegoda, N. B.; Szlachcic, A.; Guilbride, D. L.; Saibil, H. R.; Mayer, M. P.; Bukau, B. Human Hsp70 Disaggregase Reverses Parkinson's-Linked α-Synuclein Amyloid Fibrils. *Mol. Cell* **2015**, *59* (5), 781−793.
(32) Fontaine, S. N.; Zheng, D.; Sabbagh, J. J.; Martin, M. D.; Chaput, D.; Darling, A.; Trotter, J. H.; Stothert, A. R.; Nordhues, B. A.; Lussier, A.; Baker, J.; Shelton, L.; Kahn, M.; Blair, L. J.; Stevens, S. M.; Dickey, C. A. DnaJ/Hsc70 chaperone complexes control the extracellular release of neurodegenerative-associated proteins. *EMBO J.* **2016**, *35* (14), 1537−1549.
(33) Gezen-Ak, D.; Yurttaş, Z.; Çamoğlu, T.; Dursun, E. Could Amyloid-β 1−42 or α-Synuclein Interact Directly with Mitochondrial DNA? A Hypothesis. *ACS Chem. Neurosci.* **2022**, *13* (19), 2803−2812.
(34) Zhao, Q.; Luo, T.; Gao, F.; Fu, Y.; Li, B.; Shao, X.; Chen, H.; Zhou, Z.; Guo, S.; Shen, L.; Jin, L.; Cen, D.; Zhou, H.; Lyu, J.; Fang, H. GRP75 Regulates Mitochondrial-Supercomplex Turnover to Modulate Insulin Sensitivity. *Diabetes* **2022**, *71* (2), 233−248.
(35) Honrath, B.; Metz, I.; Bendridi, N.; Rieusset, J.; Culmsee, C.; Dolga, A. M. Glucose-regulated protein 75 determines ER-mitochondrial coupling and sensitivity to oxidative stress in neuronal cells. *Cell Death Discovery* **2017**, *3* (1), 17076.
(36) Wardelmann, K.; Rath, M.; Castro, J. P.; Blümel, S.; Schell, M.; Hauffe, R.; Schumacher, F.; Flore, T.; Ritter, K.; Wernitz, A.; Hosoi, T.; Ozawa, K.; Kleuser, B.; Weiß, J.; Schürmann, A.; Kleinridders, A. Central acting hsp10 regulates mitochondrial function, fatty acid metabolism, and insulin sensitivity in the hypothalamus. *Antioxidants* **2021**, *10* (5), 711.
(37) Schopf, F. H.; Biebl, M. M.; Buchner, J. The HSP90 chaperone machinery. *Nat. Rev. Mol. Cell Biol.* **2017**, *18* (6), 345−360.
(38) Falsone, S. F.; Kungl, A. J.; Rek, A.; Cappai, R.; Zangger, K. The molecular chaperone Hsp90 modulates intermediate steps of amyloid assembly of the Parkinson-related protein α-synuclein. *J. Biol. Chem.* **2009**, *284* (45), 31190−31199.
(39) Zou, J.; Guo, Y.; Guettouche, T.; Smith, D. F.; Voellmy, R. Repression of heat shock transcription factor HSF1 activation by HSP90 (HSP90 complex) that forms a stress-sensitive complex with HSF1. *Cell* **1998**, *94* (4), 471−480.
(40) McFarland, N. R.; Dimant, H.; Kibuuka, L.; Ebrahimi-Fakhari, D.; Desjardins, C. A.; Danzer, K. M.; Danzer, M.; Fan, Z.; Schwarzschild, M. A.; Hirst, W.; McLean, P. J. Chronic Treatment with Novel Small Molecule Hsp90 Inhibitors Rescues Striatal Dopamine Levels but Not α-Synuclein-Induced Neuronal Cell Loss. *PLoS One* **2014**, *9* (1), No. e86048.
(41) Gezen-Ak, D.; Dursun, E.; Hanağası, H.; Bilgiç, B.; Lohman, E.; Araz, Ö. S.; Atasoy, İ. L.; Alaylıoğlu, M.; Önal, B.; Gürvit, H.; Yılmazer, S. BDNF, TNFα, HSP90, CFH, and IL-10 Serum Levels in Patients with Early or Late Onset Alzheimer's Disease or Mild Cognitive Impairment. *J. Alzheimer's Dis.* **2013**, *37* (1), 185−195.
(42) Gustin, J. K.; Moses, A. V.; Früh, K.; Douglas, J. L. Viral Takeover of the Host Ubiquitin System. *Front. Microbiol.* **2011**, *2*, 161.
(43) Ihse, E.; Yamakado, H.; van Wijk, X. M.; Lawrence, R.; Esko, J. D.; Masliah, E. Cellular internalization of alpha-synuclein aggregates by cell surface heparan sulfate depends on aggregate conformation and cell type. *Sci. Rep.* **2017**, *7* (1), 9008.
(44) Dursun, E.; Gezen-Ak, D.; Yilmazer, S. A Novel Perspective for Alzheimer's Disease: Vitamin D Receptor Suppression by Amyloid-β and Preventing the Amyloid-β Induced Alterations by Vitamin D in Cortical Neurons. *J. Alzheimer's Dis.* **2011**, *23* (2), 207−219.
(45) Volpicelli-Daley, L. A.; Luk, K. C.; Lee, V. M.-Y. Addition of exogenous α-synuclein preformed fibrils to primary neuronal cultures to seed recruitment of endogenous α-synuclein to Lewy body and Lewy neurite-like aggregates. *Nat. Protoc.* **2014**, *9* (9), 2135−2146.
(46) Alaylıoğlu, M.; Keskin, E.; Şengül, B.; Dursun, E.; Gezen-Ak, D. A Novel and Robust Protocol for Differentiation of SH-SY5Y Neuroblastoma Cells into Neuron Like Cells. *Arch. Neuropsychiatry* **2023**.
(47) Brahic, M.; Bousset, L.; Bieri, G.; Melki, R.; Gitler, A. D. Axonal transport and secretion of fibrillar forms of α-synuclein, Aβ42 peptide and HTTExon 1. *Acta Neuropathol.* **2016**, *131* (4), 539−548.
(48) Şengül, B.; Dursun, E.; Verkhratsky, A.; Gezen-Ak, D. Overexpression of α-Synuclein Reorganises Growth Factor Profile of Human Astrocytes. *Mol. Neurobiol.* **2021**, *58* (1), 184−203.

https://doi.org/10.1021/acsomega.3c10036
ACS Omega 2024, 9, 17185−17194

(49) Dursun, E.; Gezen-Ak, D.; Yilmazer, S. A New Mechanism for Amyloid-β Induction of iNOS: Vitamin D-VDR Pathway Disruption. *J. Alzheimer's Dis.* **2013**, *36* (3), 459−474.

https://doi.org/10.1021/acsomega.3c10036
ACS Omega 2024, 9, 17185−17194